Available online at www.sciencedirect.com
SCIENCE DIRECT®
Acta Materialia 52 (2004) 1711–1720
Acta MATERIALIA
www.actamat-journals.com

Strengthening and softening mechanisms in nanocrystalline materials under superplastic deformation

M.Yu. Gutkin *, I.A. Ovid'ko, N.V. Skiba

Institute of Problems of Mechanical Engineering, Russian Academy of Sciences, Bolshoj 61, Vasil. Ostrov, St. Petersburg 199178, Russia

Received 4 August 2003; received in revised form 27 November 2003; accepted 11 December 2003

Abstract

A theoretical model is suggested which describes the strengthening and softening mechanisms in nanocrystalline materials under high-strain-rate superplastic deformation. In the framework of the model, the strengthening occurs due to the effects of triple junctions of grain boundaries (GBs) as obstacles for GB sliding. Deformation-induced migration of GBs and their triple junctions gives rise to local softening in nanocrystalline samples under superplastic deformation. With representations of the model, dependences of the yield stress on parameters characterizing the geometry of triple junctions and plastic strain degree are revealed. The results of the model account for experimental data for nanocrystalline materials exhibiting superplasticity, reported in the literature.
© 2003 Acta Materialia Inc. Published by Elsevier Ltd. All rights reserved.

Keywords: Deformation; Grain boundaries; Dislocations; Nanostructures

1. Introduction

Nanocrystalline materials exhibit unique mechanical properties representing the subject of intensive fundamental research and opening a range of new applications; see, e.g. [1–3]. Nanocrystalline materials are often extremely hard and brittle, but several examples of substantial ductility under mechanical load have been reported. Some nanocrystalline alloys even exhibit superplasticity at relatively high strain rates and low temperatures, which is characterized by very high flow stresses and the strengthening at the first extensive stage of deformation [4–12]. In other words, such nanocrystalline materials are simultaneously superplastic and superstrong. Very high values of the flow stress and the strengthening at the extensive stage of deformation are the specific features of superplastic nanocrystalline materials, distinguishing their deformation behavior from that of conventional microcrystalline materials exhibiting superplasticity. These features are the subject of growing fundamental interest [4–12] motivated by a range of new commercial applications based on use of superplasticity of nanocrystalline materials.

After the first extensive stage of superplastic deformation characterized by strengthening, the second stage occurs which is characterized by both softening and plastic flow localization and ends by failure [6–12]. Very large values of the flow stress as well as the strengthening and softening effects in nanocrystalline materials under superplastic deformation can be naturally attributed to the action of grain boundaries (GBs) whose volume fraction is extremely high in such materials. This statement is in agreement with the generally accepted view (see, e.g. [1–24]) that GBs and their triple junctions crucially affect the outstanding mechanical properties of nanocrystalline materials. High-density ensembles of GBs serve as obstacles for conventional dislocation slip in nanocrystalline materials and, at the same time, open up several effective deformation modes that usually are not significant in coarse-grained polycrystals. These modes are GB diffusional creep [13–15], triple junction diffusional creep [16], rotational mode (occurring via movement of GB disclinations) [17–20], and GB sliding [20–24]. In particular, GB sliding is considered to be the dominant mode of superplasticity in nanocrystalline materials [10–12], in which case the unusual

* Corresponding author. Tel.: +7-812-3214764; fax: +7-812-3214771.
E-mail address: gutkin@def.ipme.ru (M.Yu. Gutkin).

1359-6454/$30.00 © 2003 Acta Materialia Inc. Published by Elsevier Ltd. All rights reserved.
doi:10.1016/j.actamat.2003.12.014

strengthening and very high values of the flow stress should be related to the specific peculiarities of the GB sliding in nanocrystalline materials. The strengthening effect occurring due to transformations of GB dislocations at triple junctions has been briefly discussed in Letter [25]. The main aim of this paper is to suggest a theoretical model describing in detail both the strengthening and softening mechanisms in nanocrystalline materials under superplastic deformation as being related to transformations of GB dislocations, GBs and their triple junctions.

2. Transformations of GB dislocations at triple junctions – Model

Let us consider evolution of GB defects in a nanocrystalline solid under mechanical load. GBs with excess density of GB dislocations – carriers of GB sliding – often exist in as-fabricated nanocrystalline materials; see, e.g., [1,6]. When a mechanical load is applied to the specimen, mobile GB dislocations (with Burgers vector being parallel to GB planes) move causing GB sliding (Fig. 1(a)). They are stopped at triple junctions of GBs, where GB planes are curved and thereby dislocation movement is hampered (Fig. 1(a)). In general, GB dislocations stopped near a triple junction are capable of overcoming the junction obstacle and enter a dislocation reaction when the shear stress reaches some critical value. In nanocrystalline materials with their high-density ensembles of triple junctions, the critical shear stress needed for GB dislocations to overcome triple junctions specifies the contribution of GB sliding to the yield stress. Following [10–12], we assume that GB sliding is the dominant mode of superplasticity, in which case the critical shear stress causes the flow stress of superplastic deformation in nanocrystalline materials. With GB sliding playing the role of the dominant deformation mode of superplasticity, dependences of the critical stress on parameters of defect structures and their evolution with plastic strain in nanocrystalline materials exhibiting high-strain-rate superplasticity are responsible for the basic peculiarities of their superplastic flow.

In this paper we will calculate such dependences in the framework of the first approximation model describing transformations of GB dislocations at triple junctions. To do this, let us consider a model configuration of GB dislocations in a nanocrystalline material, which is formed near a triple junction under the action of shear stress τ applied to a nanocrystalline solid (Fig. 1(a)). The configuration consists of two GB dislocations with Burgers vectors $\mathbf{b}_1$ and $-\mathbf{b}_2$ parallel to the corresponding GB planes adjacent to the triple junction. GB dislocations are stopped by the triple junction (Fig. 1(a)) when $\tau < \tau_1^{\mathrm{crit}}$. In order to estimate the yield stress for GB sliding, we analyze the energy characteristics of transformations of GB dislocations, occurring at the triple junction. In doing so, it should be noted that an elementary act of the GB sliding is a transfer of the GB dislocation with Burgers vector $-\mathbf{b}_2$ across a triple junction (Fig. 1(b)). This transfer over a short distance l_2 becomes energetically favorable at a critical shear stress τ_1^{crit}. The transfer is accompanied by a dislocation

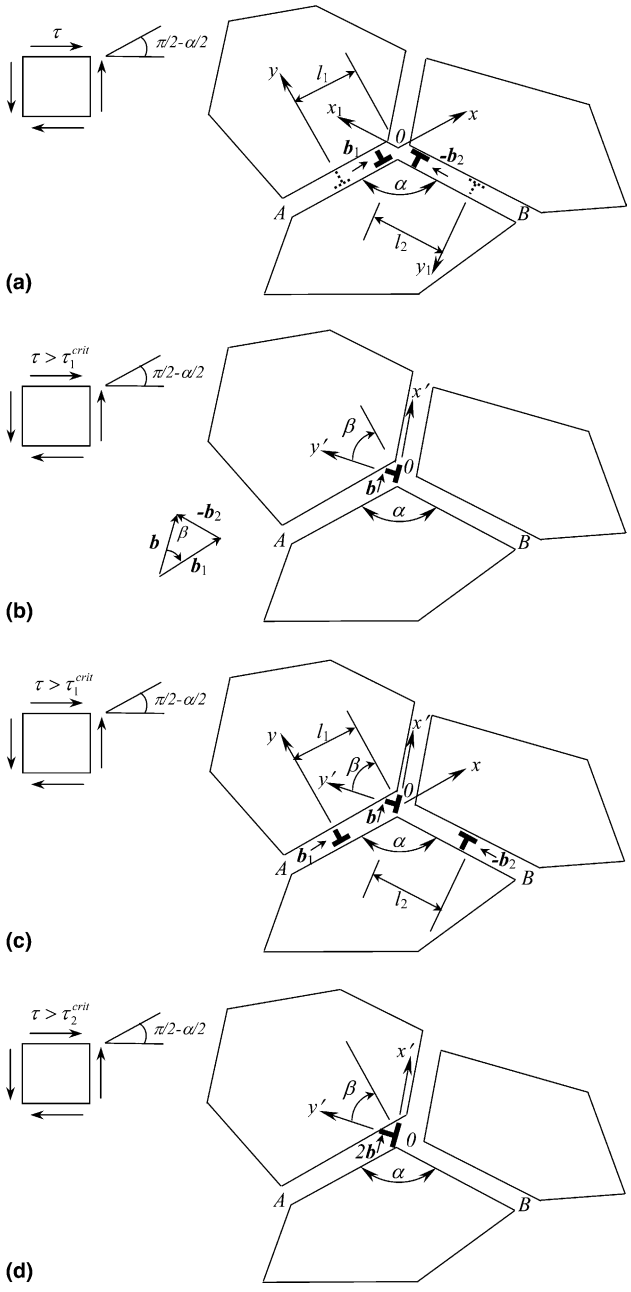

Fig. 1. Transformations of GB dislocations near a triple junction. (a) Initial (0th) state of defect configuration. Two gliding GB dislocations move towards the triple junction O. (b) Sessile dislocation with the Burgers vector $\mathbf{b}$ is formed. Triple junction is displaced by the vector $\mathbf{b}_2$ from its initial position shown in (a). (c) Generation of two new gliding GB dislocations that move towards the triple junction. (d) New sessile dislocation is formed. The triple junction is transferred by the vector $2\mathbf{b}_2$ from its initial position shown in (a).

reaction which involves the GB dislocations with Burgers vectors $\mathbf{b}_1$ and $-\mathbf{b}_2$ and results in both the formation of a sessile GB dislocation with Burgers vector $\mathbf{b} = \mathbf{b}_1 - \mathbf{b}_2$ and a displacement of the triple junction by vector $\mathbf{b}_2$ (Fig. 1(b)). In the framework of our model, the process discussed is an elementary act of superplastic deformation of a nanocrystalline specimen under mechanical load.

After the dislocation reaction (Fig. 1(a) and (b)) at the triple junction has occurred, the two new GB dislocations are generated, say, as those resulted from dissociation of lattice dislocations trapped by GBs. The new GB dislocations move under the action of the shear stress towards the triple junction (Fig. 1(c)). (For simplicity, hereafter, we assume that all moving GB dislocations at boundary AO (OB, respectively) are characterized by a Burgers vector having the magnitude b_1 ($-b_2$ respectively). For brevity, here and in the following we shall refer to GB dislocations with Burgers vector magnitudes b_1 and b_2 as b_1- and b_2-dislocations, respectively.) These moving b_1- and b_2-dislocations interact elastically with the sessile GB dislocation which obstructs the movement of the new dislocations. At the stress level $\tau_2^{\mathrm{crit}} > \tau_1^{\mathrm{crit}}$, a new elementary act of GB sliding at the triple junction occurs. With the Burgers vector conservation law, the elementary act results in both the formation of a new sessile dislocation and a new displacement of the triple junction by $\mathbf{b}_2$ (Fig. 1(d)). The new and pre-existing sessile dislocations converge resulting in the formation of a new sessile dislocation with Burgers vector being tentatively equal to $2\mathbf{b} = 2(\mathbf{b}_1 - \mathbf{b}_2)$ (Fig. 1(d)).

The process under consideration occurs repeatedly, which is accompanied by an increase of the Burgers vector of the sessile dislocation at each step. Since the sessile dislocation obstructs the moving GB dislocations, the critical shear stress increases with evolution of the defect structure. We think that it is this phenomenon which is responsible for strengthening detected experimentally [6–12] in nanocrystalline materials under superplastic deformation (occurring mostly through the GB sliding).

In addition to the formation of the sessile GB dislocations with growing Burgers vectors, the transformations of GB dislocations at triple junction give rise to displacements of the triple junction (Figs. 1 and 2). More precisely, in our model, n elementary acts of GB sliding at the triple junction cause the junction displacement by $n\mathbf{b}_2$ (Fig. 2). To accommodate this displacement, local GB migration can occur as shown in Fig. 2. In doing so, the local GB migration is driven by a decrease of the total length of the GBs and the corresponding decrease of the GB energy. The migration leads to an increase of the triple junction angle α (Fig. 2) that characterizes the triple junction as a geometric obstacle for GB sliding. With rising the number n of

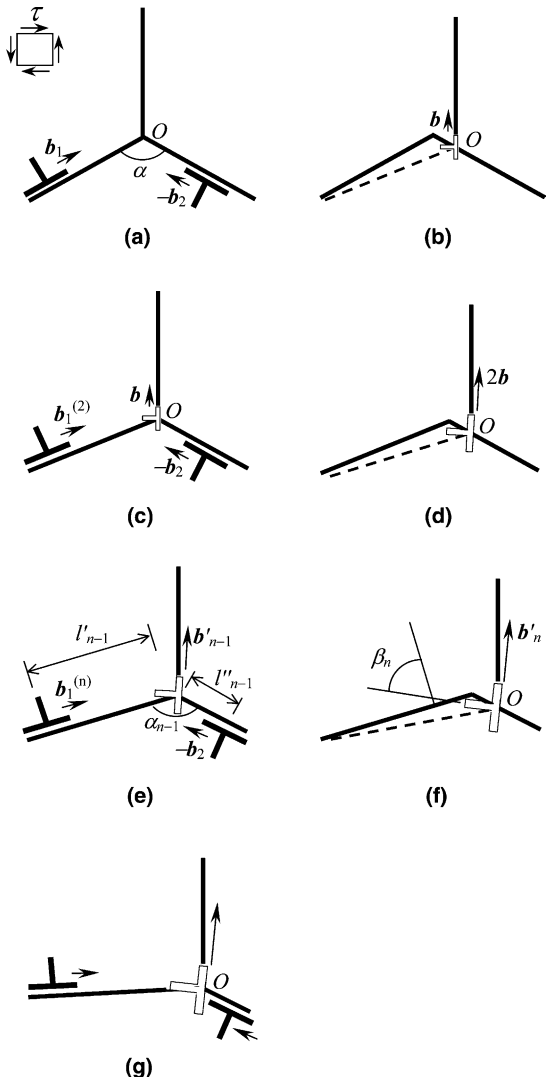

Fig. 2. Numerous acts of transfer of GB dislocations across a triple junction and accompanying local migration of GBs make GB planes (adjacent to the triple junction) to be temporarily parallel to each other.

elementary acts of GB sliding through the triple junction (Fig. 2), the triple junction angle α increases; it tends to reach value of 180° at which GB planes AO and OB are parallel. In these circumstances, the strengthening effect of the triple junction as a geometric obstacle for GB sliding decreases with rising the number n.

Also, the triple junction angle α strongly influences the elastic interaction (attraction) between GB dislocations that glide along GB planes AO and OB towards each other (Figs. 1 and 2). More precisely, when the triple junction angle α increases, so does the elastic attraction force between the gliding dislocations that carry GB sliding along GB planes AO and OB; for quantitative details, see Section 3. This factor leads to a decrease of the shear stress needed to provide GB sliding, if the triple junction angle α grows parallel with GB sliding (Fig. 2). Thus, both the GB-sliding-induced

displacement of the triple junction and accompanying GB migration (Fig. 2) cause the softening effect in nanocrystalline materials.

The strengthening effect related to GB dislocation storage at triple junctions (Figs. 1 and 2) and the softening effect related to GB migration in vicinities of triple junctions (Fig. 2) are in competition. This competition is responsible for the typical character of "stress–strain" dependence in nanocrystalline materials under high-strain-rate superplastic deformation. In short, the strengthening effect is dominant during the first extended stage of superplastic deformation, while the softening effect becomes essential during the second stage of superplastic deformation which ends by failure. These effects and their competition will be analysed in detail in the next sections.

3. Energy characteristics of transformations of GB dislocations at triple junctions

3.1. The first transformation event

Let us consider the energy characteristics of the first event of transformation of GB dislocations at a triple junction (Fig. 1(a) and (b)), which occurs under the action of a shear stress τ. The first transformation is characterized by the difference $\Delta W_1 = W_1 - W_0$ between the energies of the final (W_1) and initial (W_0) states of the defect configuration, shown in Fig. 1(b) and (a), respectively. The transformation in question is energetically favorable (unfavorable), if $\Delta W_1 < 0$ ($\Delta W_1 > 0$, respectively). The equation $\Delta W_1 = 0$ gives a set of critical values of parameters for the defect configuration, at which its transformation becomes energetically favorable.

The initial defect configuration represents two gliding GB dislocations stopped near a triple junction (Fig. 1(a)). Its energy W_0 consists of three terms:

$$W_0 = E_{\text{self}}^{b_1} + E_{\text{self}}^{b_2} + E_0^{b_1-b_2}, \tag{1}$$

where $E_{\text{self}}^{b_1}$ and $E_{\text{self}}^{b_2}$ are the self-energies of the b_1- and $-b_2$-dislocations, respectively, and $E_0^{b_1-b_2}$ is the energy that characterizes the elastic interaction between these dislocations.

The self-energies are given by the standard formula (e.g., [26]) as follows:

$$E_{\text{self}}^{b_i} = \frac{Db_i^2}{2}\left(\ln\frac{R}{r_{c_i}} + 1\right), \tag{2}$$

where $D = G/[2\pi(1-\nu)]$, G denotes the shear modulus, ν the Poisson ratio, r_{c_i} the cut-off radius of the stress field of the b_1- and $-b_2$-dislocations, for $i = 1$ and 2, respectively, and R the screening length of the dislocation long-range stress field.

The energy of elastic interaction between two defects can be calculated as the work spent to transfer one defect from a free surface of a solid to its current position in the stress field created by the other defect [27]. In this approach, in our case with two GB dislocations (Fig. 1(a)), their interaction energy $E_0^{b_1-b_2}$ can be calculated using the formula:

$$E_0^{b_1-b_2} = -b_1\int_{-R}^{0}\tau_{xy}^{b_2}(x, y=0)\mathrm{d}x, \tag{3}$$

where $\tau_{xy}^{b_2}$ is the shear stress which is induced by the $-b_2$-dislocation and acts on the b_1-dislocation. This stress is written as follows:

$$\tau_{xy}^{b_2}(x,y) = \frac{1}{2}\left(\sigma_{x_1x_1}^{b_2} - \sigma_{y_1y_1}^{b_2}\right)\sin 2\alpha + \sigma_{x_1y_1}^{b_2}\cos 2\alpha, \tag{4}$$

where the dislocation stress field components $\sigma_{x_1x_1}^{b_2}$, $\sigma_{y_1y_1}^{b_2}$ and $\sigma_{x_1y_1}^{b_2}$ are written in the coordinate system Ox_1y_1 associated with the $-b_2$-dislocation and rotated by an angle α relative to the coordinate system Oxy associated with the b_1-dislocation (Fig. 1(a)). These components are given by the well known formulas [26] as:

$$\begin{aligned}
\sigma_{x_1x_1}^{b_2} &= -Db_2\frac{y_1\left(y_1^2+3x_1^2\right)}{\left(x_1^2+y_1^2\right)^2},\\
\sigma_{y_1y_1}^{b_2} &= Db_2\frac{y_1\left(x_1^2-y_1^2\right)}{\left(x_1^2+y_1^2\right)^2},\\
\sigma_{x_1y_1}^{b_2} &= Db_2\frac{x_1\left(x_1^2-y_1^2\right)}{\left(x_1^2+y_1^2\right)^2}.
\end{aligned} \tag{5}$$

In formulas (5), the coordinates (x_1y_1) are in the following relationships with the coordinates (x, y):

$$\begin{aligned}
x_1 &= -(x-x_0)\cos\alpha + (y+y_0)\sin\alpha,\\
y_1 &= (x-x_0)\sin\alpha + (y+y_0)\cos\alpha,
\end{aligned} \tag{6}$$

where $x_0 = l_1 - l_2\cos\alpha$, $y_0 = l_2\sin\alpha$. With formulas (5) and (6), substitution of (4) in formula (3) yields:

$$\begin{aligned}
E_0^{b_1-b_2} = Db_1b_2\Bigg\{&\frac{1}{2}\cos\alpha\ln\left(1+\frac{R^2+2R(l_1-l_2\cos\alpha)}{l_1^2+l_2^2-2l_1l_2\cos\alpha}\right)\\
&-\frac{l_1l_2\sin^2\alpha}{l_1^2+l_2^2-2l_1l_2\cos\alpha}\\
&+\frac{2l_2(R+l_1)\sin^2\alpha}{R^2+2R(l_1-l_2\cos\alpha)+l_1^2+l_2^2-2l_1l_2\cos\alpha}\Bigg\}.
\end{aligned} \tag{7}$$

The energy of the defect configuration in its final state (Fig. 1(b)) consists of three terms:

$$W_1 = E_{\text{self}}^{b} + W_{\text{b}} + A_\tau, \tag{8}$$

where E_{self}^{b} denotes the self-energy of the sessile GB dislocation with Burgers vector $\mathbf{b}$, W_{b} the energy barrier for movement of the $-b_2$-dislocation across the triple junction, and A_τ the work of the shear stress τ, spent to transfer the b_1-dislocation over the distance l_1 and the $-b_2$-dislocation over the distance l_2.

The self-energy of the sessile dislocation is given by the standard formula [26] (similar to formula (2)):

$$E^{b}_{\text{self}} = \frac{Db^2}{2}\left(\ln\frac{R}{r_c}+1\right). \tag{9}$$

The energy barrier for GB dislocation movement across the triple junction is assumed to be $W_b = Gb_2^2\kappa$, where κ is the adjusting parameter being of the order of unity.

The work of the shear stress, spent to transfer the GB dislocations is written in the standard way as:

$$A_\tau = \tau(b_1 l_1 + b_2 l_2)\cos\alpha. \tag{10}$$

From Fig. 1(a) and (b) it follows that the Burgers vector magnitude b characterizing the sessile dislocation is related to the magnitudes, b_1 and b_2, of the Burgers vectors of the moving GB dislocations through

$$\begin{cases} b_1 = -b_2\cos\alpha + b\cos\beta, \\ b_2\sin\alpha = b\sin\beta, \end{cases} \tag{11}$$

where β is the angle by which the coordinate system (x', y') associated with the sessile dislocation is rotated relative to the coordinate system (x, y) associated with the moving b_1-dislocation (Fig. 1(b)). Relations (11) can be re-written in the following form:

$$\beta = \operatorname{arc\,ctg}(b_1/b_2\,\mathrm{cosec}\alpha + \operatorname{ctg}\alpha), \tag{12}$$

$$b = b_2\sin\alpha\,\mathrm{cosec}\beta. \tag{13}$$

With formulas (1), (2), (7)–(10) and (12), we find the expression for the characteristic energy difference $\Delta W_1 = W_1 - W_0$:

$$\begin{aligned}\Delta W_1 = {} & Gb_2^2\kappa + \tau(b_1 l_1 + b_2 l_2)\cos\alpha \\ & + \frac{D}{2}\left\{(b^2 - b_1^2 - b_2^2)\left(\ln\frac{R}{r_c}+1\right)\right. \\ & - b_1 b_2\left[\cos\alpha\ln\left(1+\frac{R^2+2R(l_1-l_2\cos\alpha)}{l_1^2+l_2^2-2l_1l_2\cos\alpha}\right)\right. \\ & + \frac{l_1 l_2\sin^2\alpha}{l_1^2+l_2^2-2l_1l_2\cos\alpha} \\ & \left.\left. - \frac{4l_2(R+l_1)\sin^2\alpha}{R^2+2R(l_1-l_2\cos\alpha)+l_1^2+l_2^2-2l_1l_2\cos\alpha}\right]\right\},\end{aligned} \tag{14}$$

where the approximation $r_{c_i} \approx r_c$ was used.

The energy difference ΔW_1 has been analysed numerically in dependence on the applied shear stress τ for different values of the angle α and the following values of the model parameters: $l_1 = l_2 = 100b$, $R = 10^2 b$, and $\kappa = 1$ (Fig. 3). As is seen from the plots, ΔW_1 decreases with both τ and α. It is positive (i.e. the transformation is energetically unfavorable) for relatively small values of τ and α, and negative (i.e. the transformation is favorable) for their large values. When $\alpha \leqslant 100°$, an extremely high ($> G/50$) shear stress needs to be applied to make the transformation energetically favorable. When $\alpha \geqslant 140°$, the first transformation event is favorable even without external stress (of course, provided the GB dislocations already exist near the triple junction). In the intermediate range of α (here for $\alpha = 120°$), it is enough to apply some reasonable critical shear stress (here $\approx G/1000$) to activate the first transformation event. It is also evident that the level of the critical stress increases with decreasing α.

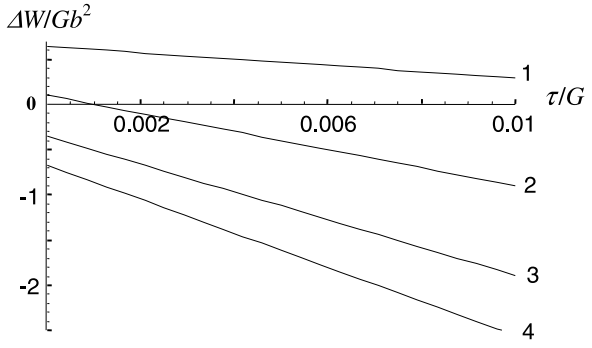

Fig. 3. The energy difference ΔW_1 vs. the applied shear stress τ for the different values of the angle $\alpha = 100°$ (1), 120° (2), 140° (3) and 160° (4), and the following values of the model parameters: $l_1 = l_2 = 100b$, $R = 10^3 b$, and $\kappa = 1$.

3.2. The nth transformation event

Now let us examine the energy characteristics of the transformation from the $(n-1)$th state of the defect system to its nth state or, in other words, the nth act of superplastic deformation (GB sliding) occurring at a triple junction (for illustration, see Fig. 2 (e) and (f)). The defect system in its $(n-1)$th state (Fig. 2(e)) consists of the sessile superdislocation characterized by Burgers vector $\mathbf{b}'_{n-1}$ and two gliding GB dislocations with Burgers vectors $\mathbf{b}_1^{(n)}$ and $-\mathbf{b}_2$, respectively. These gliding dislocations are located, respectively, at the distances l'_{n-1} and l''_{n-1} from the triple junction characterized by angle α_n (Fig. 2(e)).

We assume that the gliding GB dislocations are generated at either triple junctions A and B adjacent to the junction O or at some GB dislocation sources at the boundaries AO and OB, with the same spacing from the triple junctions A and B, respectively. With this assumption, geometric parameters, l'_{n-1}, l''_{n-1} and α_n, are related to the geometric parameters, l_1, l_2 and α, of the defect system in its initial (the 0th) state shown in Fig. 1(a) as follows (for details, see Appendix A):

$$l'^2_n = l_1/d\left(d^2 + n^2b_2^2 - 2nb_2 d\cos\alpha\right)^{1/2}, \tag{15}$$

$$l''_n = l_2 - nb_2, \tag{16}$$

$$\alpha_n = \arccos\left(\frac{n^2b_2^2 - nb_2 d + d(d-nb_2)\cos\alpha}{(d^2+n^2b_2^2-2nb_2d\cos\alpha)^{1/2}(d-nb_2)}\right). \tag{17}$$

The Burgers vector magnitude b'_n and angle β_n that characterize the sessile superdislocation in the nth state (Fig. 2(f)) are obtained from formulas (12) and (13) as follows:

$$\beta_n = \operatorname{arc\,ctg}(b_1/b_2 \operatorname{cosec}\alpha_n + \operatorname{ctg}\alpha_n), \tag{18}$$

$$b'_n = b_2 \sum_{i=1}^{n} \sin\alpha_i \operatorname{cosec}\beta_i. \tag{19}$$

The transformation in question (Fig. 2(e) and (f)) is characterized by the difference $\Delta W_n = W_n - W_{n-1}$ in the energy between the nth (W_n) and $(n-1)$th (W_{n-1}) states of the defect system. The transformation is energetically favorable, if $\Delta W_n < 0$. The set of critical parameters, including the critical shear stress for the GB sliding across the triple junction in the nth event of superplastic deformation (GB sliding) is derived from the equation $\Delta W_n = 0$.

The energy W_{n-1} (per unit length of a GB dislocation) consists of six terms:

$$W_{n-1} = E_{\text{self}}^{b_1^{(n)}} + E_{\text{self}}^{b_2} + E_{\text{self}}^{b'_{n-1}} + E_{n-1}^{b_1^{(n)}-b_2} + E_{n-1}^{b_1^{(n)}-b'_{n-1}} + E_{n-1}^{b_2-b'_{n-1}}, \tag{20}$$

where $E_{\text{self}}^{b_1^{(n)}}$, $E_{\text{self}}^{b_2}$ and $E_{\text{self}}^{b'_{n-1}}$ are the self-energies of the GB dislocations with Burgers vectors $\mathbf{b}_1^{(n)}$, $-\mathbf{b}_2$ and $\mathbf{b}'_{n-1}$, respectively, $E_{n-1}^{b_1^{(n)}-b_2}$ is the energy that characterizes interaction between mobile dislocations with Burgers vectors $\mathbf{b}_1^{(n)}$ and $-\mathbf{b}_2$, and $E_{n-1}^{b_1^{(n)}-b'_{n-1}}$ ($E_{n-1}^{b_2-b'_{n-1}}$, respectively) is the energy of the interaction of the dislocation characterized by Burgers vector $\mathbf{b}_1^{(n)}$ (dislocation characterized by Burgers vector $-\mathbf{b}_2$, respectively) with the sessile dislocation characterized by Burgers vector $\mathbf{b}'_{n-1}$.

The self-energies $E_{\text{self}}^{b_1^{(n)}}$, $E_{\text{self}}^{b_2}$ are given by formula (2), with equation $b_1 = b_1^{(n)}$ taken into consideration. The self-energy $E_{\text{self}}^{b'_{n-1}}$ is defined from formula (9), with b replaced with b'_{n-1}:

$$E_{\text{self}}^{b'_{n-1}} = \frac{Db'^2_{n-1}}{2}\left(\ln\frac{R}{r'_{c_{n-1}}} + 1\right). \tag{21}$$

The interaction energy $E_{n-1}^{b_1^{(n)}-b_2}$ is given by formula (7), with the following replacements taken into account:

$$E_{n-1}^{b_1^{(n)}-b_2} = E_0^{b_1-b_2}(\alpha \to \alpha_{n-1}, l_1 \to l'_{n-1}, l_2 \to l''_{n-1}). \tag{22}$$

The interaction energies $E_{n-1}^{b_1^{(n)}-b'_{n-1}}$ and $E_{n-1}^{b_2-b'_{n-1}}$ are calculated in the same way as the energy $E_0^{b_1-b_2}$ (see formulas (3)–(7)). In doing so, after some algebra, we get:

$$E_{n-1}^{b_1-b'_{n-1}} = Db_1 b'_{n-1}\cos\beta_{n-1}\ln\left(\frac{R}{l'_{n-1}} + 1\right), \tag{23}$$

$$E_{n-1}^{b_2-b'_{n-1}} = Db_2 b'_{n-1}\cos(\alpha_{n-1} - \beta_{n-1})\ln\left(\frac{R}{l''_{n-1}} + 1\right). \tag{24}$$

The energy of the defect configuration formed after n transfers of GB dislocations across the triple junction (Fig. 2(f)) is

$$W_n = E_{\text{self}}^{b'_n} + W_{\text{b}} + A_\tau, \tag{25}$$

where $E_{\text{self}}^{b'_n}$ is the self-energy of the sessile dislocation with Burgers vector $\mathbf{b}'_n$ (Fig. 2(f)). It is given by the following formula derived from formula (9) with b replaced with b'_n:

$$E_{\text{self}}^{b'_n} = \frac{Db'^2_n}{2}\left(\ln\frac{R}{r'_{c_n}} + 1\right). \tag{26}$$

The terms W_{b} and A_τ are defined and calculated in the same way as the corresponding terms in the energy W_1 (see formula (8)).

With formulas (2), (7), (10), (20)–(26), we find the following expression for the characteristic energy difference $\Delta W_n (= W_n - W_{n-1})$:

$$\begin{aligned}
\Delta W_n = \frac{D}{2}\Bigg\{ & b'^2_n\left(\ln\frac{R}{r'_{c_n}} + 1\right) - b'^2_{n-1}\left(\ln\frac{R}{r'_{c_{n-1}}} + 1\right) \\
& - (b_1^2 + b_2^2)\left(\ln\frac{R}{r_c} + 1\right) \\
& - b_1 b_2\Bigg[\cos\alpha_{n-1}\ln\left(1 + \frac{R^2 + 2R(l'_{n-1} - l''_{n-1}\cos\alpha_{n-1})}{l'^2_{n-1} + l''^2_{n-1} - 2l'_{n-1}l''_{n-1}\cos\alpha_{n-1}}\right) \\
& + \frac{l'_{n-1}l''_{n-1}\sin^2\alpha_{n-1}}{l'^2_{n-1} + l''^2_{n-1} - 2l'_{n-1}l''_{n-1}\cos\alpha_{n-1}} \\
& - \frac{4l''_{n-1}(R + l'_{n-1})\sin^2\alpha_{n-1}}{R^2 + 2R(l'_{n-1} - l''_{n-1}\cos\alpha_{n-1}) + l'^2_{n-1} + l''^2_{n-1} - 2l'_{n-1}l''_{n-1}\cos\alpha_{n-1}}\Bigg] \\
& - 2b'_{n-1}\Bigg[b_1\cos\beta_{n-1}\ln\left(\frac{R}{l'_{n-1}} + 1\right) \\
& + b_2\cos(\alpha_{n-1} - \beta_{n-1})\ln\left(\frac{R}{l''_{n-1}} + 1\right)\Bigg]\Bigg\} \\
& + Gb_2^2\kappa + \tau(b_1 l'_{n-1} + b_2 l''_{n-1})\cos\alpha_{n-1}.
\end{aligned} \tag{27}$$

4. Shear stress, strengthening and softening in nanocrystalline materials

Let us calculate the shear stress τ_n^{crit} needed for the nth act of superplastic deformation to occur at the triple junction O (Fig. 2(e) and (f)), that is, the $-b_2$-dislocation to move across the triple junction containing a sessile dislocation characterized by Burgers vector $\mathbf{b}'_{n-1}$. This stress can be found from the condition that $\Delta W_n = 0$ yielding:

$$\tau_n^{\text{crit}} = \frac{E_{\text{self}}^{b'_{n-1}} - E_{\text{self}}^{b'_n} + E_{\text{self}}^{b_1^{(n)}} + E_{\text{self}}^{b_2} + E_{n-1}^{b_1^{(n)}-b_2} + E_{n-1}^{b_1^{(n)}-b'_{n-1}} + E_{n-1}^{b_2-b'_{n-1}} - W_b}{(b_1 l'_{n-1} + b_2 l''_{n-1})\cos\alpha_{n-1}}. \tag{28}$$

With the above formula, we have numerically calculated the dependence of τ_n^{crit} on n, for the following characteristic values of the system parameters: $G = 70$ GPa, $\nu = 0.3$, $b_1 = b_2 = r_c = 0.1$ nm, $r'_n = b'_n$, $R = 100$ nm. The parameter κ entering W_{b} is assumed to be 1.75.

We have considered the two cases with $l_1 = l_2 = l = d$ and $l_1 = l_2 = l < d$, where d is the length of the GBs adjacent to the triple junction O. In the former case, gliding GB dislocations are generated at the triple junctions A and B and move towards the triple junction O. This case is realized, for instance, if two sources of lattice dislocations operate in grain interiors and provide the lattice dislocation flow in certain slip systems from grain interiors to the boundaries AA' and BB' as shown in Fig. 4(a). The trapped dislocations split into GB dislocations that climb towards the triple junctions A and B (Fig. 4(b)) where these GB dislocations split into sessile and gliding GB dislocations (Fig. 4(c)).

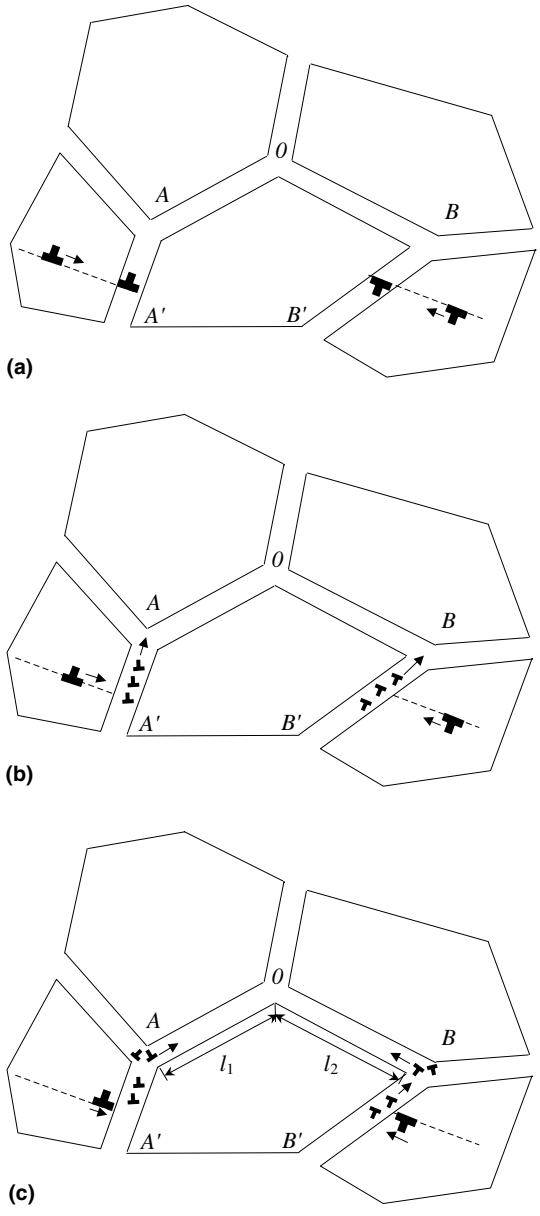

Fig. 4. Generation of GB dislocations at the triple junctions A and B. (a) Lattice dislocations move under mechanical load in grain interiors and arrive at the GBs AA' and BB'. (b) Dislocations trapped at the GBs split into GB dislocations that climb towards the triple junctions A and B. (c) Dislocation reactions at the triple junctions A and B result in the formation of gliding and sessile GB dislocations.

The second case with $l_1 = l_2 = l < d$ is realized, for instance, if two sources of lattice dislocations operate in grain interiors and provide the lattice dislocation flow in two certain slip planes from grain interiors to boundaries AO and OB as shown in Fig. 5(a). The transformations of the trapped dislocations (Fig. 5(b)) result, in particular, in the formation of gliding GB dislocations that move towards the triple junction O.

The numerically calculated dependence $\tau_n^{\mathrm{crit}}(n)$, for $l_1 = l_2 = l = d$ and different values of the triple junction angle α, are presented in Fig. 6. With rising n, τ_n^{crit} first grows, then reaches its maximum value and eventually drops off (Fig. 6). The maximum values, for $\alpha \approx 150°$ and 160°, are close to 1.2 and 0.6 GPa, respectively; these values correspond to experimental data [5,10,12] on maximum flow stresses in nanocrystalline Ni_3Al alloys under high-strain-rate superplastic deformation. The parameter n, the number of elementary acts of superplastic deformation (GB sliding) occurring at a triple junction, serves as a characteristic of the amount of local plastic strain at this triple junction. In this context, the dependence of τ_n^{crit} on n (Fig. 6) is found to have the same character as the experimentally ob-

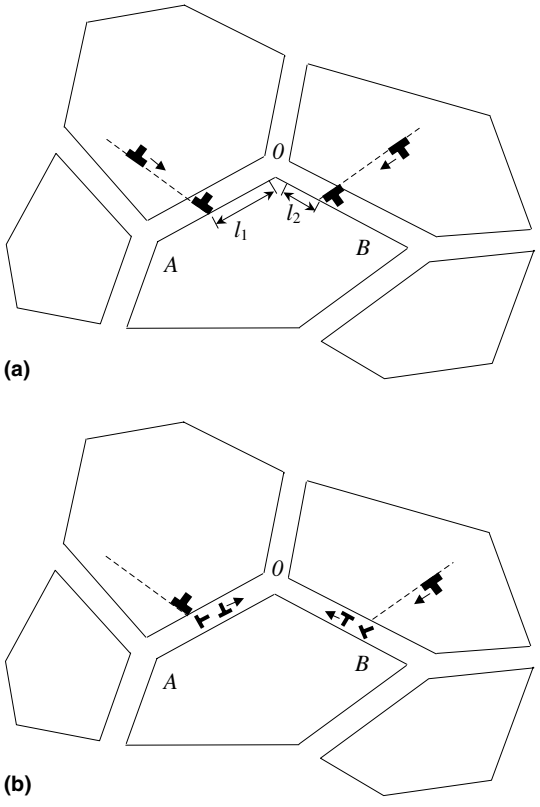

Fig. 5. Generation of gliding dislocations at the GBs AO and OB. (a) Lattice dislocations move under mechanical load in grain interiors and arrive at the GBs AO and OB. (b) Dislocations trapped at the GBs split into sessile and gliding GBs.

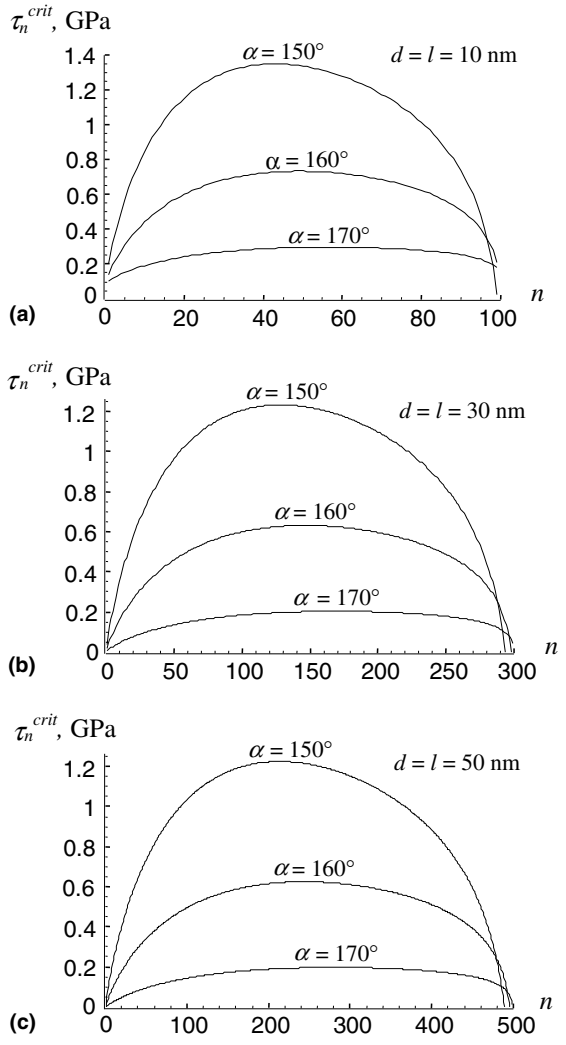

Fig. 6. Dependence of the critical shear stress τ_n^{crit} on n, the number of superplastic deformation acts occurring at the triple junction, for $l_1 = l_2 = l = d$ and different values of the system parameters.

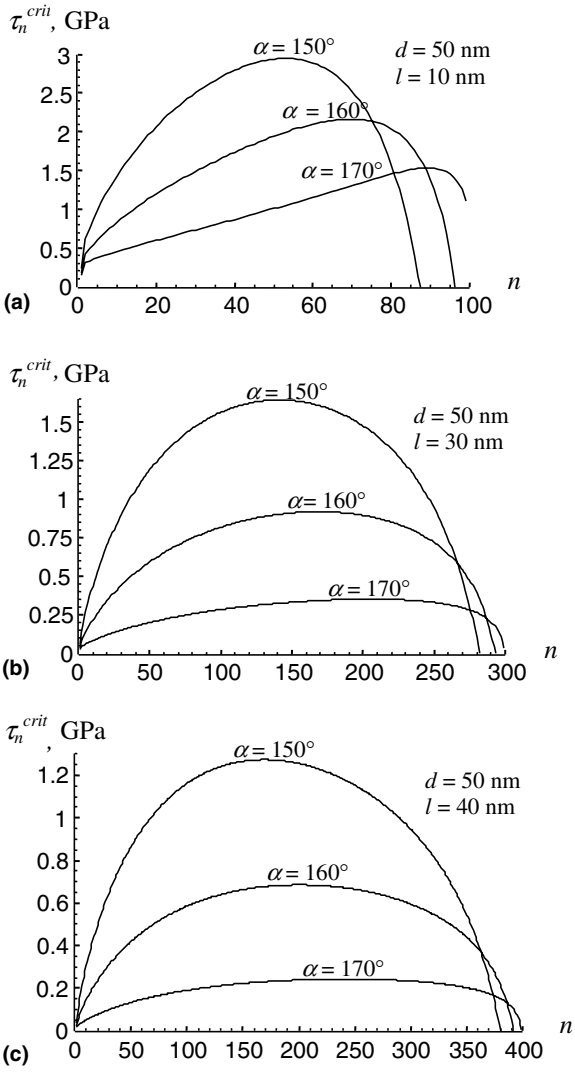

Fig. 7. Dependence of the critical shear stress τ_n^{crit} on n, the number of superplastic deformation acts occurring at triple junction, for $l_1 = l_2 = l < d$ and different values of the system parameters.

served [6–12] "flow stress–strain" dependences in real nanocrystalline materials under superplastic deformation. In particular, the growth of τ_n^{crit} with rising n obtained with our model (Fig. 6) explains the experimentally observed strengthening in superplastically deformed nanocrystalline materials, which distinguishes their deformation behavior from that of conventional microcrystalline materials exhibiting superplasticity with no strain hardening.

The numerically calculated dependences $\tau_n^{\text{crit}}(n)$, for $l_1 = l_2 = l < d$ and different values of the triple junction angle α, are presented in Fig. 7. These dependences show the same behavior as those in Fig. 6 and experimentally measured [6–12] "flow stress–strain" curves in nanocrystalline materials under superplastic deformation.

Thus, the critical shear stress τ_n^{crit} is highly sensitive to both the amount of plastic strain characterized by n and the triple junction geometry characterized by the triple junction angle α. It is illustrated by dependences presented in Figs. 6 and 7, which have the same character as the measured "flow stress–strain" curves [6–12].

The mean number $\langle n \rangle$ of elementary acts of GB sliding through one triple junction specifies the contribution of GB sliding to total plastic deformation of a nanocrystalline specimen. Indeed, the ratio nb_2/d may be treated as plastic shear strain localized at the triple junction. Let $\langle d \rangle$ denote the mean grain size. In these circumstances, the amount ε_{gb} of the plastic strain conducted by GB sliding is in the following approximate relationship with $\langle n \rangle, \langle d \rangle$ and the mean magnitude $\langle b_2 \rangle$ of Burgers vectors of GB dislocations that carry GB sliding: $\varepsilon_{\text{gb}} \approx \langle n \rangle \langle b_2 \rangle / \langle d \rangle$. For the characteristic values of $\langle b_2 \rangle = 0.1$ nm and $\langle d \rangle = 50$ nm, we have $\varepsilon_{\text{gb}} \approx 2 \times 10^{-3} \langle n \rangle$. This approximate relationship allows us to estimate the contribution of GB sliding to the total

plastic strain ε of a nanocrystalline specimen. In doing so, with experimentally measured values of $\varepsilon \approx 1.5$–2 [5,10,12] for nanocrystalline Ni_3Al alloys and dependences $\tau_n^{crit}(n)$ calculated above (see Figs. 6 and 7), we find that GB sliding provides the amount $\varepsilon_{gb} \approx 0.5\varepsilon$–$0.7\varepsilon$.

Our estimate is rather rough. To quantitatively describe the contribution of GB sliding to high-strain-rate superplastic deformation of nanocrystalline materials and calculate the corresponding "flow stress–strain" curves, it is needed to take into consideration the contributions of alternative deformation modes (different from GB sliding) to plastic flow, distributions in grain size and triple junction angle, plastic flow inhomogeneities and other factors coming into play in deformed nanocrystalline materials. A cumbersome analysis of these factors is beyond the scope of this paper focused on a first approximation description of the strengthening and softening mechanisms for high-strain-rate superplasticity exhibited by the nanocrystalline matter. The analysis of the above mentioned factors will be the subject of further theoretical investigations of authors, based on the results reported here.

5. Discussion and concluding remarks

In this paper, it has been shown theoretically that superplastic deformation, occurring by GB sliding in nanocrystalline materials, is characterized by both strengthening due to transformations of gliding GB dislocations at triple junctions and softening due to local migration of triple junctions and adjacent GBs (Figs. 1 and 2). Our theoretical analysis of the energy characteristics of the transformations indicates that the transformations of GB dislocations at triple junctions are energetically favorable in certain ranges of parameters of the defect configuration (Fig. 3). The corresponding flow stress is caused mostly by the critical shear stress τ_n^{crit} which is highly sensitive to both the level of plastic strain characterized by n and the triple junction geometry characterized by triple junction angle α; see Figs. 6 and 7. The formation of sessile GB dislocations at triple junctions (Figs. 1 and 2) causes a strengthening effect that dominates at the first long stage of superplastic deformation. At the same time, the movement of GB dislocations across triple junctions can be accompanied with GB migration driven by a decrease of the total length and thereby energy of GBs (Fig. 2). As a result of numerous acts of movement of GB dislocations across triple junctions and the accompanying GB migration, the GB planes temporarily become parallel to each other at the shear surface (Fig. 2). In these circumstances, triple junctions stop being geometric obstacles for the movement of new GB dislocations, which, therefore, is enhanced along the shear surface. The enhancement of GB sliding due to local migration of GBs was discussed in papers [21,22] focused on a qualitative description of this phenomenon. Here we have calculated the dependence of τ_n^{crit} on n for different values of the triple junction angle α (Figs. 6 and 7), which quantitatively characterizes the softening related to local migration of GBs and their triple junctions in a mechanically loaded nanocrystalline material. The discussed representations on the softening mechanism related to local migration of GBs (see papers [21,22] and analysis given in this paper) are supported by experimental observation [28,29] of plastic flow localization in nanocrystalline materials. Following electron microscopy experiments [28,29], shear bands where superplastic flow is localized in nanocrystalline materials contain brick-like grains with GBs being parallel and perpendicular to the shear direction. It is effectively and naturally interpreted as a result of the GB migration (Fig. 2) accompanying GB sliding across triple junctions.

Thus, with results of our calculations of the critical shear stress $\tau_n^{crit}(n)$ (see Section 4), there are both the strengthening and the softening effects occurring due to transformations of GB dislocations at triple junctions and the accompanying local migration of GBs, respectively. The competition between the strengthening and the softening effects is capable of crucially influencing the deformation behavior of nanocrystalline materials exhibiting high-strain-rate superplasticity. In particular, superplastic deformation regime is realized if the strengthening dominates over the softening during the first extensive stage of deformation (characterized by a plastic strain of hundreds of percent). This strengthening prevents the necking and is responsible for an increase of the flow stress that drives the movement of GB dislocations (see Figs. 6 and 7). With rising plastic strain, local GB migration (Fig. 2) makes GB planes to be tentatively parallel to each other in some local regions of a loaded sample. As a result, local softening becomes substantial, which causes gradual macroscopic softening inherent in the second stage of superplastic deformation of nanocrystalline materials.

At some level of plastic strain, the softening becomes dominant over the strengthening. At this point, movement of new GB dislocations is dramatically enhanced along the shear surfaces where GB planes temporarily become parallel to each other due to movement of previous GB dislocations across their junctions. As a corollary, the softening effect leads to plastic flow localization and neck formation followed by failure.

Acknowledgements

This work was supported, in part, by the Office of US Naval Research (grant N00014-01-1-1020), the Russian

Fund of Basic Research (grant 01-02-16853), Russian State Research Program on Solid-State Nanostructures, Russian Academy of Sciences Program "Structural Mechanics of Materials and Construction Elements", St. Petersburg Scientific Center, and "Integration" Program (grant B0026).

Appendix A

The geometry of migrating triple junction O and its adjacent GBs AO and OB is presented in Fig. 8. With this figure and elementary trigonometry (theorem of cosines), we find the following relationships between the geometric parameters shown in Fig. 8:

$$\begin{cases} L^2 = 2d^2(1-\cos\alpha), \\ L^2 = d'^2 + (d-nb)^2 - 2d'(d-nb)\cos\alpha_n, \\ d'^2 = d^2 + n^2b^2 - 2dnb\cos\alpha. \end{cases} \tag{A.1}$$

From the system of Eq. (A.1) we have the expression for $\cos\alpha_n$:

$$\cos\alpha_n = \frac{n^2b_2^2 - nb_2d + d(d-nb_2)\cos\alpha}{(d^2 + n^2b_2^2 - 2nb_2d\cos\alpha)^{1/2}(d-nb_2)}. \tag{A.2}$$

With formula (A.2), we find formula (17) for the triple junction angle α_n in the nth state of the defect system under consideration.

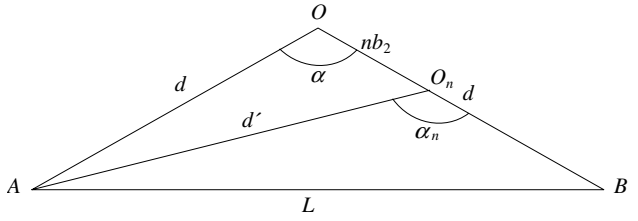

Fig. 8. Geometry of a triple junction that migrates from the position O to the position O_n, and its adjacent GBs AO (AO_n) and OB (O_nB).

References

[1] Mohamed FA, Li Y. Mater Sci Eng A 2001;298:1.
[2] Padmanabhan KA. Mater Sci Eng A 2001;304–306:200.
[3] Koch CC, Morris DG, Lu K, Inoue A. MRS Bull 1999;24:54.
[4] Mishra RS, Valiev RZ, McFadden SX, Mukherjee AK. Mater Sci Eng A 1998;252:174.
[5] McFadden SX, Misra RS, Valiev RZ, Zhilyaev AP, Mukherjee AK. Nature 1999;398:684.
[6] Islamgaliev RK, Valiev RZ, Mishra RS, Mukherjee AK. Mater Sci Eng A 2001;304–306:206.
[7] Mishra RS, Valiev RZ, McFadden SX, Islamgaliev RK, Mukherjee AK. Phil Mag A 2001;81:37.
[8] Mishra RS, Stolyarov VV, Echer C, Valiev RZ, Mukherjee AK. Mater Sci Eng A 2001;298:44.
[9] Valiev RZ, Song C, McFadden SX, Mukherjee AK, Mishra RS. Phil Mag A 2001;81:25.
[10] Mukherjee AK. Mater Sci Eng A 2002;322:1.
[11] Valiev RZ, Alexandrov IV, Zhu YT, Lowe TC. J Mater Res 2002;17:5.
[12] Mukherjee AK. In: Mishra RS, Earthman JC, Raj SV, editors. Creep deformation: fundamentals and applications. Warrendale: TMS; 2002. p. 3–19.
[13] Masumura RA, Hazzledine PM, Pande CS. Acta Mater 1998;46:4527.
[14] Kim HS, Estrin Y, Bush MB. Acta Mater 2000;48:493.
[15] Yamakov V, Wolf D, Phillpot SR, Gleiter H. Acta Mater 2002;50:61.
[16] Fedorov AA, Gutkin M, Yu, Ovid'ko IA. Scr Mater 2002;47:51.
[17] Murayama M, Howe JM, Hidaka H, Takaki S. Science 2002;295:2433.
[18] Ovid'ko IA. Science 2002;295:2386.
[19] Gutkin MYu, Kolesnikova AL, Ovid'ko IA, Skiba NV. Phil Mag Lett 2002;81:651.
[20] Gutkin MYu, Ovid'ko IA, Skiba NV. Acta Mater 2003;51:4059.
[21] Hahn H, Mondal P, Padmanabhan KA. Nanostruct Mater 1997;9:603.
[22] Hahn H, Padmanabhan KA. Phil Mag B 1997;76:559.
[23] Konstantinidis DA, Aifantis EC. Nanostruct Mater 1998;10:1111.
[24] Fedorov AA, Gutkin MYu, Ovid'ko IA. Acta Mater 2003;51:887.
[25] Gutkin MYu, Ovid'ko IA, Skiba NV. J Phys D: Appl Phys 2003;36:L47.
[26] Hirth JP, Lothe J. Theory of dislocations. Wiley: New York; 1982.
[27] Mura T. In: Herman H, editor. Advances in material research, vol. 3. New York: Interscience; 1968. p. 1–108.
[28] Wei Q, Jia D, Ramesh KT, Ma E. Appl Phys Lett 2002;81:1240.
[29] Jia D, Ramesh KT, Ma E. Acta Mater 2003;51:3495.